Charging Oriented Sensor Placement and Flexible Scheduling in Rechargeable WSNs

Tao Wu*[†], Panlong Yang*, Haipeng Dai[‡], Wanru Xu[†], Mingxue Xu*

*School of Computer Science and Technology, University of Science and Technology of China

[†]College of Communication Engineering, Army Engineering University of PLA

[‡]State Key Laboratory for Novel Software Technology, Nanjing University, Nanjing, Jiangsu 210024, China
Email: {terence.taowu,xwr88023}@gmail.com, plyang@ustc.edu.cn, haipengdai@nju.edu.cn, xmx18@mail.ustc.edu.cn

Abstract—The recent breakthrough in Wireless Power Transfer (WPT) provides a promising way to support rechargeable sensors to enrich a series of energy-consuming applications. Unfortunately, two major design restrictions hinder the applicability of rechargeable sensor networks. First, most of the sensor placement schemes are focusing on the sensing tasks instead of the charging utility, which leaves a considerably high performance gap towards the optimal result. Second, the charging scheduling is non-flexible, where full or nothing charging policy suffers from the relatively low charging coverage as well as efficiency. In this paper, we focus on how to efficiently improve the charging utility when introducing charging oriented sensor placement and flexible scheduling policy. To this end, we jointly consider optimizing node positions and charging allocations. In particular, we formulate a general convex optimization problem under a general routing constraint, which generates great difficulty. We utilize area partition and charging discretization methods to reformulate a submodular function maximization problem. Thus a constant approximation algorithm is delivered to construct a near optimal charging tour. To this end, we analyze the performance loss from the discretization to guarantee that the output of the proposed algorithm has more than $(1-\varepsilon)/4(1-1/e)$ of the optimal solution, where ε is an arbitrarily small positive parameter $(0 \le \varepsilon \le 1)$. Both simulations and field experiments are conducted to evaluate the performance of our proposed algorithm.

I. INTRODUCTION

Varies types of sensor devices such as WISP RFID tags are organized into an autonomous network to sense, monitor, process and deliver information to enrich a series of energy-consuming applications. Sustained energy furnish is essential to support energy-critical sensors to execute tasks. Fortunately, the recent breakthroughs in Wireless Power Transfer (WPT) can provide continuous and reliable power supply for these rechargeable sensors without replacing their batteries which needs extensive human efforts. Exploiting the WPT technique helps construct a rechargeable wireless sensor network, where rechargeable sensors can harvest energy conveniently from a mobile charger traveling in the network [1].

Unfortunately, two major design restrictions hinder the applicability of rechargeable sensor networks. First, most of the sensor placement schemes are focusing on the sensing tasks instead of the charging utility [2] [3]. They usually give priority to sensing tasks such as the target coverage or event detection while overlooking the location of the power resource. However, it is somehow unfavorable that charging some remote sensors would incur too much energy waste

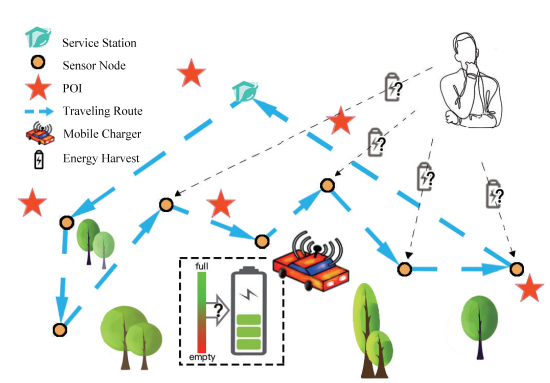


Fig. 1: Scenario of mobile charging for POIs coverage

and charging delay due to the far traveling. Many literatures have studied efficient mobile charging scheduling to meet the energy requirements of sensors. For example, Shi *et al.* [4] first analyzed the charging requirements to construct a Hamiltonian cycle. Some other perspectives have also been discussed such as charging delay minimization [5], charging or network utility maximization [6]–[8], on-demand charging requests [9]–[13], *etc.* However, there still leaves a considerably high performance gap towards the optimized charging utility.

Second, previous charging scheduling is usually non-flexible, where full or nothing charging policy suffers from the relatively low charging coverage as well as efficiency. The direct policy loses the degree of freedom for energy allocation and may degrade energy utilization efficiency for task execution. As one task can be cooperated by multiple sensors to accomplish tasks, the full charging may increase the energy consumption because of the possible spatial redundance of sensors [14] [15]. Therefore, the overall charging utility may decline when only considering sensing tasks and full or nothing charging policy.

In this paper, we focus on how to efficiently improve the charging utility when introducing charging oriented sensor placement and flexible scheduling policy. Formally, we jointly consider optimizing node positions and charging allocations respecting the charging utility. In particular, we formulate a general convex optimization problem under the general routing constraint. In our charging scenario as shown in Fig. 1, target distribution information is given in the sensing region. The expected charging utility is quantified by the effectiveness of covering target/POI (Point of Interest) by sensors which is

related to the sensing distance and harvested energy. Thus we should determine sensor positions and the amount of harvested energy, such that the overall charging utility is maximized.

Our proposed convex optimization problem under the routing constraint generates great difficulty which includes three technical challenges. First, the charging utility is nonlinear with distance as sensors can be deployed in the continuous space and have infinite candidate locations. Second, selecting sensors for full or nothing charging has been generally NP-hard. Then combining the flexible energy allocation policy would induce extra nonlinearity which forms a complex mixed integer problem. Third, it would be more complicated when considering tour scheduling and thus poses another great challenge.

To tackle aforementioned challenges, we partition the whole square area into many subareas and descretize the charging energy to construct enough virtual sensors in one grid. Then we transform the initial problem into a combinatorial problem, where we analyze the influence of discretization granularity on the optimality of required solution. After proving the submodular property of the reformulated objective function, a constant approximation algorithm is delivered to calculate sensor positions and energy allocation strategy to maximize the overall charging utility. Our contributions can be summarized as follows:

- We present the first step on proposing a charging oriented sensor placement and flexible scheduling policy to enhance the overall charging utility.
- We reduce candidate locations from infinite to finite with bounded partition error ε and prove the 1/2 gap of charging discretization. We transform the complicated convex optimization problem subject to a general routing constraint into a submodular function maximizing problem, which has $(1-\varepsilon)/4(1-1/e)$ approximation ratio.
- We carry out our policy in both Matlab and TX91501 power transmitters, and both simulations and field experiments are conducted to evaluate the performance of our propose algorithm.

The rest of the paper is organized as follows. We review related works in Section II. Then, we present the system model and formulate the problem in Section III. The specific solution is presented in Section IV and we analyze the theoretical results in Section V. In Section VI and Section VII, we present the results of simulations and experiments respectively. Finally, we conclude the work in Section VIII.

II. RELATED WORK

Although static chargers scheduling is an essential issue to be considered, which including some studies on power allocation [16] and safe charging [17]–[19], etc. We present more research on mobile charging to illustrate the novelty of our work. These existing works usually focused on the fixed sensor placement to schedule mobile charging. Fu et al. [5] studied to determine the mobile charger stop locations and durations to minimize the total charging delay. Shi et al. [4] employed a mobile charger to periodically charge the given

TABLE I: Definition of notations

Notation	Definition
o_j, O	a POI, POI set
m	Number of POIs
s_i, S	Sensor, sensor set
$u(s_i, o_j)$	Utility of s_i by on o_j
e_i	Amount of charged energy for s_i
E	Energy capacity sensors
$d(s_i, o_j)$	Distance between s_i and o_j
D	Farthest coverage distance of a sensor
$f_{S'}(o_j)$	Additive calculated utility of set S' on o_j
$U_{S'}(o_j)$	Utility of set S' on POI o_j
$U_{threshold}$	Utility threshold on o_j
U(S')	Overall charging utility with respect to S'
$P_{S'}$	Position set of deployed sensors S'
$\mathcal{L}(P_{S'})$	Closed charging tour including $P_{S'}$
Budget	Limited energy capacity of the mobile charger
$C^{travel}(S')$	Traveling energy consumption with respect to S'
C(S')	Overall energy consumption with respect to S'
$\lambda, \alpha, c_1, c_2$	Constant parameters

sensors to maximize the charger's vacation time. Shu *et al.* [20] first studied controlling traveling velocity of the mobile charger for the time-bounded charging scenario. Dong *et al.* [21] also optimize the charger's velocity to meet a feasible task assignment. Zhong *et al.* [22] considered the dynamic energy consumption of sensors. Jiang *et al.* [23] investigated the event monitoring applications when scheduling mobile chargers in an on-demand way.

Some existing works considered partial charging. Liang *et al.* [7] studied the charging utility maximization problem while sensors can be full or partial charged. They also extended to a general case where multiple sensors can be charged simultaneously [8]. Dai *et al.* also applied partial charging policy to maximize the overall charging utility when considering EMR safety [24] and charging direction [25]. However, none of them considered charging task oriented sensor placement and flexible scheduling policy jointly.

III. SYSTEM MODEL AND PROBLEM FORMULATION

A. Network Model

We consider m logical and substantial POIs denoted as $O = \{o_1, o_2, ... o_m\}$ distributed in the 2D plane. Let $S = \{s_1, s_2, ... s_n\}$ be the set of rechargeable sensors which can be deployed anywhere to sense, monitor and collect the information of these POIs. A mobile charger with a limited energy capacity would start from the service station, visit these sensors to transfer power wirelessly and return to the depot before the energy is exhausted. Definition of notations is listed in Table I.

When considering the charging utility, we measure the utility of deploying one sensor in terms of POI coverage effectiveness. The coverage effectiveness of each sensor is independent and only related to its location and flexible harvested energy. To define the charging utility, we use the empirical coverage model [3] as follows:

$$u(s_i, o_j) = \begin{cases} \frac{\lambda e_i}{(d(s_i, o_j) + \alpha)^2}, & d \le D\\ 0, & d > D, \end{cases}$$
(1)

where $u(s_i, o_i)$ represents the charging utility of sensor s_i when covering POI o_j , $d(s_i, o_j)$ is the distance between sensor s_i and POI o_i , e_i is the amount of charged energy which is adjustable, α , λ are the constants and D is the maximum coverage distance of the sensor.

The effectiveness of multiple sensors covering one single POI is additive. Then, for any selected sensor set $S' \subset S$, the additive charging utility on POI o_j can be calculated by

$$f_{S'}(o_j) = \sum_{s_i \in S'} u(s_i, o_j). \tag{2}$$

Each POI has an upper bound of coverage effectiveness which means the additive charging utility has a threshold $U_{threshold}$. Therefore, we define the final charging utility for POI o_j as

$$U_{S'}(o_j) = \min\{f_{S'}(o_j), U_{threshold}\}. \tag{3}$$

And the total charging utility can be represented by

$$U(S') = \sum_{j=1}^{m} U_{S'}(o_j). \tag{4}$$

We consider two types of energy cost for mobile charging: the traveling cost and the charging cost. Having deployed sensor s_i in the 2D plane, we can use $(x[s_i], y[s_i])$ to denote the coordinate of position p_{s_i} . Then we can calculate the Euclidean distance $|p_{s_i}p_{s_j}|:(S,S)\to \mathbf{R}$ between two sensors s_i, s_j and furthermore achieve the length of closed path including deployed sensors S'. We use coefficient c_1 to represent energy cost per unit length. Therefore, for the deployed sensor set $S' \subset S$, the traveling energy cost is given by

$$C^{Travel}(S') = c_1 \mathcal{L}(P_{S'}) = c_1 \sum_{p_{s_i}, p_{s_j} \in P} |p_{s_i} p_{s_j}|,$$

where $P_{S'}$ is the position set corresponding to deployed sensor set S'. Thus we use $\mathcal{L}(P_{S'})$ to denote the closed charging tour that starts and ends at the same depot p_{s_0} , while all sensors in S' are visited only once.

When considering the charging cost, all deployed sensors have the same battery capacity E and can be charged in a flexible way. Then we have the charging cost as $c_2 \sum_{s_i \in S'} e_i$ for S', where c_2 denotes the charging efficiency which means the

Therefore, the eventual energy cost for S' is expressed by

$$C(S') = c_1 \mathcal{L}(P_{S'}) + c_2 \sum_{s_i \in S'} e_i. \tag{5}$$
B. Problem Formulation

energy cost for per unit energy harvest.

Naturally, the mobile charger has a limited energy capacity Budget and the total amount of energy consumption should not violate the capacity constraint. Thus we have

$$c_1\mathcal{L}(P_{S'})+c_2\sum_{s_i\in S'}e_i\leq Budget. \tag{6}$$
 Our objective is to optimize the placement and flexible

charging allocation for selected sensors to construct a closed charging tour, so as to maximize the charging utility in the network. Then the problem can be formulated as a general convex optimization problem under the routing constraint:

$$\begin{aligned} & \textbf{(P1)}: \max \quad U(S') \\ & s.t. \quad c_1 \mathcal{L}(P_{S'}) + c_2 \sum_{s_i \in S'} e_i \leq Budget, \quad \forall p_{s_i} \in \Omega, S' \subseteq S. \end{aligned}$$

C. Problem Hardness Analysis

In the optimization of problem P1, the coverage utility is nonlinear with distance. We need to select partial sensors to place in the continuous space which means the candidate locations of sensors are infinite. The most straightforward method is to enumerate all possible deployed positions but may incur very high computational complexity. Even the sensor placement is given, selecting for full or nothing charging is in general NP-hard [26]. Then, considering the flexible energy allocation policy would induce extra nonlinearity, which forms a complex mixed integer problem. Moreover, it would be more complex when considering tour scheduling. It involves finding an optimal closed charging tour, similar to solving a Traveling Salesman Problem which is NP-hard [27]. Therefore, our initial problem is nonlinear as well as the combination of two NP-hard problems which shows great difficulty.

IV. SOLUTION

A. Area Partition

In this subsection, we try to reduce the number of candidate sensor positions from infinite to finite. As sensors can be deployed at any point of a given square plane $\Omega = a * a$, we first confine the deployment by partitioning the placement area into many small subareas. As show in Fig. 2, we discrete the plane Ω into uniform grids with side length δ . Suppose we have Γ number of girds denoted by $(g_1, g_2, ...g_{\Gamma})$, where $\Gamma = \left\lceil \frac{|\Omega|}{\delta^2} \right\rceil$. Next, we can approximately regard all points in the same grid are identical and the point in a grid can be randomly chosen as the candidate placement position. Naturally, the coverage effectiveness from a sensor at any location in the gird to any POI can be viewed as a constant, which is equal to that achieved from the longest distance between the grid and the POI. Taking Fig. 2 as an example, given a fixed POI o and any two sensors s_i and s'_i deployed in grid g_i respectively, the distance between sensor s_i or s'_i and POI o can be approximately equal to the longest distance $d(g_i, o)$ as shown in green line. Then we have the relationship $d(s_i, o) \approx d(s'_i, o) \approx d(g_i, o)$. Apparently, the approximated charging utility is the minimum utility that can be achieved from any sensor in the grid.

In fact, as each deployed sensor has its maximal coverage range with radius length D, it can achieve zero or non-zero utility value according to whether the distance between the sensor and the POI exceeds D or not. In Fig. 2, observing two sensor s_j and s_i' in grid g_j have $d(s_j, o) \leq D$ and $d(s'_i, o) > D$ respectively, we calculate the charging utility value $u(s_i, o) > 0$ and $u(s_i', o) = 0$ subsequently. Thus, to address the performance loss, we adopt a conservation scheme to decide the coverage distance by checking whether $d(g_i, o)$ exceeds D or not. Then we modify the utility model as follows:

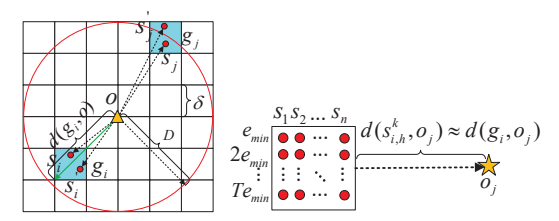


Fig. 2: Grid partition

Fig. 3: Charging Discretization

Fig. 2: Grid partition Fig. 3: Charging Discretization
$$u(g_i,o) = \begin{cases} \frac{\lambda \sum\limits_{p_{s_i} \in g_i} e_i}{(d(g_i,o) + \alpha)^2}, & d(g_i,o) \leq D \\ 0, & d(g_i,o) > D, \end{cases}$$

$$\sum_{p_{s_i} \in g_i} e_i \text{ represents the sum of harvested energy of graphle conserved deployed in grid a support of graphle conserved deployed in grid a$$

rechargeable sensors deployed in grid g_i .

We have the following lemmas for coverage distance approximation and charging utility approximation error.

Lemma 1. If $u(g_i, o) > 0$, which means the approximated charging utility from any sensor in grid g_i to POI o is greater than zero, then any sensor in grid g_i can cover POI o with the coverage distance $D - \sqrt{2}\delta$.

Lemma 2. Set

$$\delta = \frac{\sqrt{2}}{2}\alpha(\frac{1}{\sqrt{1-\varepsilon}} - 1),$$

where ε is an arbitrarily small positive parameter $(0 \le \varepsilon \le 1)$. For any sensor s_i that is deployed in the grid g_i to cover POI o, we have

$$u(s_i, o) \ge (1 - \varepsilon)u(g_i, o). \tag{8}$$

Proof: We can take δ into the utility model above and calculate the ratio $u(s_i, o)$ to $u(g_i, o)$ as

$$\frac{u(s_i,o)}{u(g_i,o)} = \left(\frac{d(g_i,o)+\alpha}{d(s_i,o)+\alpha}\right)^2 \ge \left(\frac{d(g_i,o)+\alpha}{d(g_i,o)+\sqrt{2}\delta+\alpha}\right)^2$$

$$= \left(\frac{d(g_i,o)+\alpha}{d(g_i,o)+\frac{\alpha}{\sqrt{1-\varepsilon}}}\right)^2 = (1-\varepsilon)\frac{\left(d(g_i,o)+\alpha\right)^2}{\left(\sqrt{1-\varepsilon}d(g_i,o)+\alpha\right)^2} \ge 1-\varepsilon.$$

Thus we get the result $u(s_i, o) \geq (1 - \varepsilon)u(g_i, o)$ and meanwhile have Γ uniform grids with the length δ .

B. Charging Discretization

After area partition, we have finite candidate positions for sensor placement. We emphasize that in each grid it is allowed to deploy more than one sensor, while the energy budget of the mobile charger is not violated. As deployed sensors can be flexibly charged, we presents another charging discretization method to allocate energy and approximate the charging utility, as shown in Fig. 3.

For the rechargeable sensor with a battery capacity E, we divide E into uniform T pieces and let $e_{min} = \frac{E}{T}$ be the minimum amount of energy charged to a sensor. Then for any sensor s_h that can be placed in grid g_i , T virtual copies $\{s_{i,h}^1, s_{i,h}^2, ..., s_{i,h}^T\}$ are created and each copy $s_{i,h}^k$ corresponds to ke_{min} amount of received energy. Then we have the modified utility model as follows:

$$u(s_{i,h}^k, o_j) = \begin{cases} \frac{\lambda k e_{\min}}{(d(s_{i,h}^k, o_j) + \alpha)^2}, & d(s_{i,h}^k, o_j) \le D\\ 0, & d(s_{i,h}^k, o_j) > D. \end{cases}$$
(9)

We note that although such discretization method incurs utility error, it can be bounded as shown in Lemma 4.

C. Problem Reformulation

After above approximation procedures, we have finite candidate positions for sensor placement and charging strategies for energy allocation that we can obtain $n\Gamma T$ virtual sensors X in the overall network. Similar to Equation 2, the additive utility for POI o_j is $f_{X'}(o_j) = \sum_{s_i^k, \in X'} u(s_{i,h}^k, o_j)$ and we have

the discrete utility as

$$U_{X'}(o_j) = \min\{f_{X'}(o_j), U_{threshold}\}. \tag{10}$$

Therefore the overall charging utility is $U(X') = \sum_{j=1}^{m} U_{X'}(o_j)$.

As a mobile charger needs to optimize its charging tour after sensor placement, we adopt a conservative method that uses the longest distance $d(g_i, g_j)$ between two grids (g_i, g_j) to calculate the traveling cost. Meanwhile, we approximate the distance of sensors in the same grid to be zero, while considering the bound of performance loss after area partition. Therefore, this conservative method can guarantee the energy budget constraint not be violated and we use $\mathcal{L}(P'_{X'})$ to denote the modified traveling path.

Thus the initial P1 problem can be reformulated as

(**P2**): max
$$\sum_{j=1}^{m} U_{X'}(o_j)$$
 (11)

(P2):
$$\max \sum_{j=1}^{m} U_{X'}(o_j)$$
 (11)
 $s.t. \ c_1 \mathcal{L}(P'_{X'}) + c_2 \sum_{s_{i,h}^k \in X'} ke_{min} \leq Budget, \ \forall X' \subseteq X$ (11a)

Now P2 becomes as a combinatorial optimization problem where (11a) shows more stringent constraint of the energy budget. Therefore, P2 falls into the scope of maximizing a submodular function subject to a general routing constraint. In the next section we give some preliminary definitions to assist further theoretical analysis.

D. Approximation Algorithm

The detailed algorithm for the charging maximization problem after discretization is described in Algorithm 1. We draw $\Gamma = \left\lceil \frac{|\Omega|}{\delta^2} \right\rceil$ uniform grids with the length $\delta = \frac{\sqrt{2}}{2} \alpha (\frac{1}{\sqrt{1-\varepsilon}} - 1)$. Next, the sensor energy capacity E is divided into uniform Tpieces with the minimum e_{min} amount of energy.

Therefore the main idea of the algorithm is to select the most

cost-efficient virtual sensor
$$s^*$$
 in each iteration as follows.
$$s^* = \underset{s_i^{h,k} \in X \backslash X'}{\arg\max} \frac{U(X' \cup \{s_i^{h,k}\}) - U(X')}{\hat{C}(X' \cup \{s_i^{h,k}\}) - \hat{C}(X')}. \tag{12}$$

Initially, the candidate set X has $n\Gamma T$ virtual sensors and the selected virtual sensor set X' is empty. We would calculate the marginal charging utility $U(X' \cup \{s_i^{h,k}\}) - U(X')$ according the utility model when adding a new virtual sensor $s_i^{h,k}$. Meanwhile, we calculate the marginal energy consumption $\hat{C}(X' \cup \{s_i^{h,k}\}) - \hat{C}(X')$ using an approximation cost function \hat{C} since the optimal cost is often infeasible to compute. Then we choose a fast and simple nearest neighbour rule with a $\log(n\Gamma T)$ -approximation ratio and the impact on quality of this approximation would be described in next subsection.

Algorithm 1: Approximation Algorithm

```
Input: The positions of m POIs, the number of sensors n, the
              parameters of the coverage utility model \alpha, and energy
              consumption coefficient c_1, c_2, each POI utility
    threshold U_{threshold} and energy capacity Budget. Output: The selected virtual sensor X', overall coverage utility
                 U(X').
 1 Partition the given quare plane into many subareas by drawing
    \Gamma = \left\lceil \frac{|\Omega|}{\delta^2} \right\rceil \text{ uniform grids with the length } \delta = \frac{\sqrt{2}}{2} \alpha (\frac{1}{\sqrt{1-\varepsilon}} - 1).
2 Divide the sensor energy capacity E into uniform T pieces
    with the minimum amount of charged energy e_{min} = \frac{E}{T}. Then
    we have n\Gamma T virtual sensors denoted by set X.
 3 Initial: X' = \emptyset, \hat{C}(X') = 0;
    \mathcal{A} = \arg\max\{U(s_i^{h,k})|s_i^{h,k} \in X, \hat{C}(s_i^{h,k}) \le Budget\};
   while X \neq null do
          foreach s_i^{h,k} \in X do
5
                Computing marginal utility U(X' \cup \{s_i^{h,k}\}) - U(X')
 6
                and marginal traveling energy consumption
                \hat{C}(X' \cup \{s_i^{h,k}\}) - \hat{C}(X') using nearest neighbour rule
                and a so-called substitute algorithm.
                 \underset{s_{i}^{h,k} \in X \backslash X'}{\arg\max} \frac{U(X' \cup \{s_{i}^{h,k}\}) - U(X')}{\hat{C}(X' \cup \{s_{i}^{h,k}\}) - \hat{C}(X')}
 7
          if \hat{C}(X' \cup \{s^*\}) \leq Budget then X' = X' \cup \{s^*\};
 8
10 if U(\mathcal{A}) \geq \mathcal{U}(\mathcal{X}') then
     X' = \mathcal{A};
12 Output X', U(X');
```

Since the charging utility is approximated in a grid by area partition, all sensors in the grid would be charged successfully as long as the traveling path of the mobile charger intersects with the grid. Then after using the nearest neighbour rule to achieve the approximated tour, we use a substitute algorithm to shorten the tour further which is detailed in Algorithm 2. The progress of iteration terminates until violating the budget of the mobile charger $\hat{C}(X' \cup \{s^*\}) \leq Budget$. Upon obtaining X', we compare U(X') with $U(\mathcal{A})$ which selects the single sensor and choose the maximal one in the end.

Substitute algorithm: Supposing that utilizing the nearest neighbour rule helps acquire γ grids $\{g_1', g_2', ..., g_\gamma'\}$ in order and we connect their respective center points $p_1, p_2, ..., p_\gamma$ to construct the initial closed tour $\mathcal{L}(P)$. Note that there may be multiple sensors deployed in a grid, we can still use one position to represent them due to the location approximation and performance loss guarantee. Then we use a binary search idea to find the substitute locations for sensors and optimize the tour iteratively.

For each point p_i in P, we try to connect p_{i-1} and p_{i+1} to construct the segment $\overline{p_{i-1}p_{i+1}}$ and check whether g_i is path-covered by $\overline{p_{i-1}p_{i+1}}$ by comparing the least distance with δ . If yes, we obtain p_i' inside $\overline{p_{i-1}p_{i+1}}$ as well as in g_i ; otherwise, we search another location p_i' inside the segment $\overline{p_ip_{i+1}}$ using binary search with a granularity control parameter σ to replace p_i , under the constraint that g_i should be path-covered by segment $\overline{p_{i-1}p_i'}$, too. In the binary search,

Algorithm 2: Substitute Algorithm

```
Input: The acquired grids set G' = \{g'_1, g_2, ..., g'_{\gamma}\}, side length
             of grid \delta, the control parameter \sigma
    Output: The shortened traveling path \mathcal{L}(P')
   for all p_i (i = 1, 2, ..., \gamma) do
 1
         Connect p_{i-1}, p_i and p_{i+1} respectively to construct the
2
         segment set C(\overline{p_{i-1}p_i}) and C(\overline{p_{i-1}p_{i+1}}).
         if all grids path-covered by C(\overline{p_{i-1}p_i}) are also
         path-covered by C(\overline{p_{i-1}p_{i+1}}) then
          P' \leftarrow Obtain p'_i in P;
 4
         else
 5
              p_s = p_i; p_t = p_{i+1};
               while |\overline{p_s p_t}| > \sigma do
 7
                    p_i' = (p_s + p_t)/2;
 8
                    if all grids in C(p_{i-1}p'_i) \cup C(p_ip'_i) are in
 9
                    C(p_{i-1}p'_i) then
                        p_s = p_i';
10
                    else
11
12
                         p_t = p_i';
                   \leftarrow replace p_i by p'_i in P;
13
```

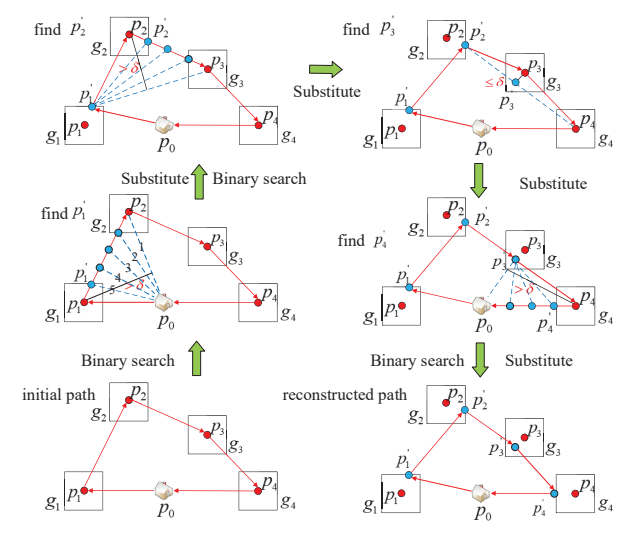


Fig. 4: Substitute process

the parameter σ is used to control the granularity of binary search. An example of Algorithm 2 is shown in Fig. 4, the traveling path is initialized to be $\{p_0, p_1, p_2, p_3, p_4, p_0\}$. The location p_1 is not path-covered by $\overline{p_0p_2}$, and thus binary search is used to find a new path $\overline{p_0p_1'}$ to substitute segment $\overline{p_0p_1}$. Specifically, path 1, 2, 3, 4, and 5 are tried and finally path 5 is chosen as it path-covers g_1 . Thus, we select the corresponding node p_1' to substitute p_1 . Using the same substitute method, we find p_2' and p_4' . We obtain p_3' because the grid p_3' is path-covered by p_2' p_4 . Finally, we find the new locations by the substitute method and therefore the traveling path is updated to $\{p_0, p_1', p_2', p_3', p_4', p_0\}$ as shown in Fig. 4.

V. THEORETICAL ANALYSIS

Definition 1: (Nonnegativity, Monotonicity, and Submodularity) Given a finite ground set \mathcal{U} , a real-valued set function defined as $f: 2^{\mathcal{U}} \to R$, f is called *nonnegative*, *monotone* (nondecreasing), and submodular if and only if it satisfies following conditions, respectively.

- $f(\emptyset) = 0$ and $f(A) \ge 0$ for all $A \subseteq \mathcal{U}$ (nonnegative);
- $f(A) \le f(B)$ for all $A \subseteq B \subseteq \mathcal{U}$ or equivalently: $f(A \cup \{e\}) f(A) > 0$ for all $A \subseteq \mathcal{U}$ and $e \in \mathcal{U} \setminus A$ (monotone);
- $f(A) + f(B) \ge f(A \cup B) + f(A \cap B)$, for any $A, B \subseteq \mathcal{U}$ or equivalently: $f(A \cup \{e\}) f(A) \ge f(B \cup \{e\}) f(B)$, $A \subseteq B \subseteq \mathcal{U}$, $e \in \mathcal{U} \setminus B$ (submodular);

Then, we have the following lemma:

Lemma 3. The objective function in **P2** is nonnegative, monotone and submodular.

Proof: Apparently, the objective function is nonnegative and monotone according to the utility model in Equation 9, 10 and 11. Given the virtual sensor subset $X'' \subset X' \subset X$, we have $U(X') \geq U(X'') \geq 0$.

To prove the submodularity, we should prove the property of diminishing marginal utility in our formulated objective function. As the coverage utility is addictive for m POIs, we only need to compare the marginal utility $\Delta_s U_{X''}(o_j) = U_{X''\cup\{s\}}(o_j) - U_{X''}(o_j)$ and $\Delta_s U_{X'}(o_j) = U_{X'\cup\{s\}}(o_j) - U_{X'}(o_j)$ of any POI o_j when adding s into X'' and X' respectively.

Considering the utility threshold $U_{threshold}$, the charging utility is

$$U_{X''}(o_j) = \min\{f_{X''}(o_j), U_{threshold}\},\tag{13}$$

$$U_{X'}(o_j) = \min\{f_{X'}(o_j), U_{threshold}\}. \tag{14}$$

- 1. If $U_{threshold} \leq f_{X''}(o_j)$, then $U_{X''}(o_j) = U_{X'}(o_j) = U_{threshold}$. The coverage utility is still $U_{threshold}$ after adding a sensor s. Thus we have $\Delta_s U_{X''}(o_j) = \Delta_s U_{X'}(o_j) = 0$.
- 2. If $f_{X''}(o_j) < U_{threshold} \leq f_{X'}(o_j)$, then $U_{X''}(o_j) = f_{X''}(o_j)$ and $U_{X'}(o_j) = U_{threshold}$. After adding a sensor s, $U_{X'' \cup \{s\}}(o_j) = \min\{f_{X'' \cup \{s\}}(o_j), U_{threshold}\}$ and $U_{X' \cup \{s\}}(o_j) = U_{threshold}$. We have

$$\Delta_s U_{X''}(o_i) - \Delta_s U_{X'}(o_i)$$

- $= \min\{f_{X'' \cup \{s\}}(o_j), U_{threshold}\} f_{X''}(o_j)$
- $= \min\{f_{X'' \cup \{s\}}(o_j) f_{X''}(o_j), U_{threshold} f_{X''}(o_j)\} \ge 0.$
- 3. If $f_{X'}(o_j) < U_{threshold} \le f_{X'' \cup \{s\}}(o_j)$, then $U_{X''}(o_j) = f_{X''}(o_j)$ and $U_{X'}(o_j) = f_{X'}(o_j)$. After adding a sensor s, $U_{X'' \cup \{s\}}(o_j) = \min\{f_{X'' \cup \{s\}}(o_j), U_j\} = U_{threshold}$ and $U_{X' \cup \{s\}}(o_j) = \min\{f_{X' \cup \{s\}}(o_j), U_{threshold}\} = U_{threshold}$. We have

$$\begin{split} & \Delta_s U_{X''}(o_j) - \Delta_s U_{X'}(o_j) \\ &= U_{threshold} - f_{X''}(o_j) - (U_{threshold} - f_{X'}(o_j)) \\ &= f_{X'}(o_j) - f_{X''}(o_j) \ge 0. \end{split}$$

 $\begin{array}{lll} \text{4. If} & f_{X'' \cup \{s\}}(o_j) < U_{threshold} \leq f_{X' \cup \{s\}}(o_j), \\ U_{X''}(o_j) &= f_{X''}(o_j) & \text{and} & U_{X'}(o_j) = f_{X'}(o_j). \\ \text{After adding a sensor} & s, & \text{we have} & U_{X'' \cup \{s\}}(o_j) = s \end{array}$

 $\min\{f_{X''\cup\{s\}}(o_j), U_{threshold}\} = f_{X''\cup\{s\}}(o_j) \text{ and } U_{X'\cup\{s\}}(o_j) = \min\{f_{X'\cup\{s\}}(o_j), U_{threshold}\} = U_{threshold}.$ We have

$$\begin{split} & \Delta_s U_{X''}(o_j) - \Delta_s U_{X'}(o_j) \\ &= f_{X'' \cup \{s\}}(o_j) - f_{X''}(o_j) - (U_j - f_{X'}(o_j)) \\ &= u(s,o_j) + f_{X'}(o_j) - U_j \\ &= f_{X' \cup \{s\}}(o_j) - U_j \geq 0. \end{split}$$

5. If $f_{X' \cup \{s\}}(o_j) < U_{threshold}$, $U_{X''}(o_j) = f_{X''}(o_j)$ and $U_{X'}(o_j) = f_{X'}(o_j)$. After adding a sensor s, we have $U_{X'' \cup \{s\}}(o_j) = \min\{f_{X'' \cup \{s\}}(o_j), U_{threshold}\} = f_{X'' \cup \{s\}}(o_j)$ and $U_{X' \cup \{s\}}(o_j) = \min\{f_{X' \cup \{s\}}(o_j), U_{threshold}\} = f_{X' \cup \{s\}}(o_j)$. Then we derive that

$$\Delta_s U_{X''}(o_j) - \Delta_s U_{X'}(o_j)$$

$$= f_{X'' \cup \{s\}}(o_j) - f_{X''}(o_j) - (f_{X' \cup \{s\}}(o_j) - f_{X'}(o_j))$$

$$= u(s, o_j) - u(s, o_j) = 0.$$

Therefore, we prove the objective function is submodular.

Lemma 4. When the mobile charger has a large energy capacity that $B > 2\sqrt{2}nc_1a$, the discrete utility after charging discretization would achieve at least 1/2 of continuous optimal charging utility.

Proof: As the mobile charger has more than $2\sqrt{2}nc_1a$ amount of energy, then it can visit all sensors at least once when traveling in the a*a square plain. We use U^* denote the continuous optimal solution where any sensor can be charged any amount of energy to maximize the overall coverage utility. Given any minimum amount of energy charged to a sensor as e_{min} , we can achieve a discrete solution U_r by rounding U^* . For example, for any sensor s_i to be charged e_i amount of energy in U^* , we round it by charging only $\left\lfloor \frac{e_i}{e_{min}} \right\rfloor e_{min}$ and thus construct this discrete solution U_r . Apparently due to $\left\lfloor \frac{e_i}{e_{min}} \right\rfloor e_{min} \leq e_i$, U_r is a feasible discrete solution.

Moveover, the sufficient energy of the mobile charger can maintain that each sensor can be charged e_{min} amount of energy. Then we consider this kind of feasible discrete solution which can be denoted by U_e . Naturally, the value of the sum of the two discrete solutions is larger than the value of the optimal solution and we have

$$U^* \le U_r + U_e. \tag{15}$$

If we use U_c^{\ast} to denote the optimal discrete solution based on the e_{min} amount of energy, apparently we have the following two relations as

$$U_r \leq U_c^*, U_e \leq U_c^*$$

and derive $U_r + U_e \le 2U_c^*$. Combining Equation 15, we have the result $U^* \le 2U_c^*$.

Theorem 1. Given the energy capacity of the mobile charger that $Budget > 2\sqrt{2}nc_1a$, the proposed algorithm achieves an approximation ratio of $(1-\varepsilon)/4(1-1/e)$ and its time complexity is $O(n\Gamma T)^2$.

Proof: From Subsection IV-C we have transformed the initial problem into maximizing a submodular function subject

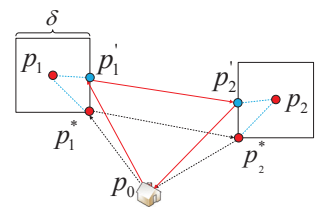


Fig. 5: Optimized tour proof

to a general routing constraint. Thus referring to [28], the iterative greedy cost-efficient algorithm would have 1/2(1 -1/e) bi-criterion approximation ratio compared to the optimal solution with a slight relaxed budget constraint. The approximated cost function \hat{C} would directly influence the relaxed decree of budget constraint. In our proposed algorithm, the nearest neighbour rule can achieve $\log(n\Gamma T)$ that guarantee the relaxed effect which can be found in [28].

Furthermore, as we set $\delta=\frac{\sqrt{2}}{2}\alpha(\frac{1}{\sqrt{1-\varepsilon}}-1)$, we have the utility error $u(s_i,o)\geq (1-\varepsilon)u(g_i,o)$ by following Lemma 2. And Lemma 4 shows the 1/2 gap between the discrete and continuous solution. Finally, the our obtained solution can achieve $(1-\varepsilon)/4(1-1/e)$ approximation ratio. Due to the $n\Gamma T$ iteration at most and $n\Gamma T$ times when using the neighbour rule to find the next virtual sensor in each iteration, therefore the overall time complexity is bounded by $O(n\Gamma T)^2$.

Lemma 5. Using $\mathcal{L}(P')$ to denote the achieved traveling path by Algorithm 2, then we can easily derive that each substitute operation reduces the traveling length by triangle inequality.

Let $\mathcal{L}(P^*)$ denote the optimal traveling path. With Lemma 5, we have the following theorem.

Theorem 2. Having achieved the approximated path $\mathcal{L}(P)$ with γ number of grids, we can obtain $|\mathcal{L}(P')| \leq |\mathcal{L}(P^*)| +$ $\sqrt{2}\gamma\delta$ by Algorithm 2 with the time complexity $O(\gamma^2\log\frac{\delta}{\sigma})$.

Proof: We denote the achieved grids to be pathcovered are $G = \{g_1, g_2, ..., g_\gamma\}$ and use $\mathcal{L}(P^*) =$ $\{p_0, p_1^*, ..., p_i^*, ..., p_\gamma^*, p_0\}$ to denote the optimal traveling path where p_0 is the start and end point. After executing Algorithm 2, we can obtain the traveling path $\mathcal{L}(P')$ = $\{p_0, p'_1, ..., p'_i, ..., p'_{\gamma}, p_0\}$ we use p_i^*, p'_i and p_i to denote the optimal stop location, the stop location obtained by Algorithm 2 and the center location in grid g_i , respectively. Then we construct an auxiliary detouring path including the optimal one to present our theoretical result.

The detour path is conducted by adding segment $\{p_i^* p_i' p_i^*\}$ into the optimal path $\mathcal{L}(P^*)$. An shown in Fig. 5, we have the optimal path $\{p_0,p_1^*,p_2^*,p_0\}$ and $\{p_0,p_1',p_2',p_0\}$ obtained by substitute method. Thus we conduct the detour traveling path as $\{p_0, p_1^*, p_1', p_1^*, p_2^*, p_2', p_2^*, p_0\}$. According to the triangle inequality, we have

$$|p_0, p_1^* p_1' p_1^*, ..., p_\gamma^* p_\gamma' p_\gamma^*, p_0| \ge |\mathcal{L}(P')|.$$

For the bounded grid, we have

$$|p_i^* p_i' p_i^*| = 2|p_i^* p_i'| \le \sqrt{2}\delta.$$

Hence

$$|p_0, p_1^* p_1' p_1^*, ..., p_{\gamma}^* p_{\gamma}' p_{\gamma}^*, p_0| \le |\mathcal{L}(P)^*| + \sqrt{2}\gamma\delta.$$

Thus, we obtain $|\mathcal{L}(P')| \leq |\mathcal{L}(P^*)| + \sqrt{2}\gamma\delta$.

Next, we investigate the complexity of Algorithm 2. It is intuitive that the time complexity consists of iterations and the substitute consumption. In that, it generates $O(\gamma)$ iterations for γ grids. In each iteration, the binary search consumes $O(\gamma \log \frac{\delta}{\sigma})$ for each substitute step. Therefore, the time complexity of substitute method is $O(\gamma^2 \log \frac{\delta}{\sigma})$.

VI. EVALUATIONS

In this section, we conduct extensive simulations to verify the performance of the proposed algorithm in terms of the error threshold ε , the budget of the mobile charger, energy discretization number, utility threshold.

A. Evaluation Setup

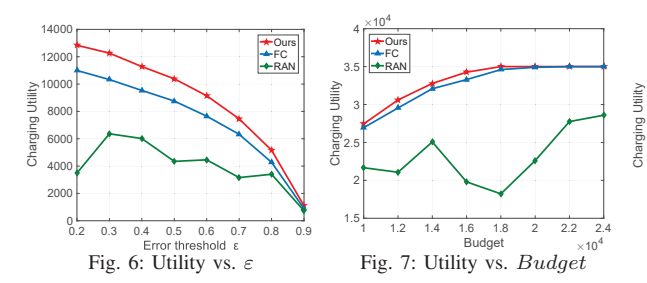
In our simulation, the sensing region is a 50m*50m square area. We use the following default setup that there are 50 POIs in the 2D plane and 20 sensors at most. The energy capacity of the mobile charger and one sensor is set as Budqet = 3000and E=80 respectively. The utility threshold of each POI is set to 700. The default error threshold ε is set as $\varepsilon = 0.8$ and the default minimum amount of charged energy $e_{min} = 4$. $\alpha = 10, c_1 = 1, c_2 = 10, \lambda = 1000.$

B. Baseline Setup

As there is no algorithm available for jointly sensor placement and mobile charging problem. We devised two algorithms named random algorithm (RAN) and full charging algorithm (FC) for comparison. RAN randomly selects a position for sensor placement and allocates random amount of energy while not violating the budget constraint at each iteration. If exceeding the budget, RAN randomly selects another position and energy allocation strategy. FC is similar to our proposed algorithm but tries to charge the placed sensor up to full energy capacity. At each iteration, FC uses a simple greedy strategy and selects the position for placement that can achieve the maximal utility.

C. Evaluation Results and Analysis

- 1) Impact of error threshold ε . Our proposed algorithm outperforms the other algorithms by at least 14.38% as the error threshold ε increases from 0.2 to 0.9. As shown in Fig. 6, all these algorithms have a diminishing trend with the error threshold ε . They decrease fast as the error threshold ε rises. This is because the utility function is inverse proportion to the distance square. Rising the error threshold ε would directly extend the side length of partitioned uniform grids according to equation $\delta=\frac{\sqrt{2}}{2}\alpha(\frac{1}{\sqrt{1-\varepsilon}}-1)$ and lead to the longer approximated coverage distance. Therefore, to reduce the running time of our algorithm, we set $\varepsilon = 0.5$ and the side length of grid $\delta = 2.93$.
- 2) Impact of the budget of the mobile charger Budget. Our proposed algorithm outperforms the other algorithms as the



budget of the mobile charger increases. Obviously, when we provide more energy for the mobile charger, the performance of all the algorithms has an increasing trend. As depicted in Fig. 7, our algorithm increase the coverage utility by 27.5% when the budget is improved from 10000 to 24000. However, it then becomes relatively stable when the budget is more than 20000. What accounts for this stability is the influence of the utility threshold. Since the utility threshold of each POI is 700 and there are 50 POIs in default, the overall coverage utility threshold is 50*700 = 35000 and increasing the budget from 20000 to 24000 would not bring external utility.

3) Impact of energy discretization number T. Our proposed algorithm outperforms the other algorithms by at least 17.5% as number of energy discretization increases from 5 to 40. From Fig. 8 we can see that the utility of our proposed algorithm has a slightly increasing trend with the number of energy discretization while FC just becomes stable. This is because FC always selects full charging mode which may incur possible waste of energy. Specifically, When additive utility on one POI o_j has grown up near to the amount of threshold $U_{threshold}$, then adding a new sensor s_i with full charging will only have a small value $U_{threshold} - u(s_i, o_j)$ of the marginal utility. The charging utility of our proposed algorithm improves because the discretization granularity provides more energy allocation strategies and would directly influence the required optimality.

4) Impact of the utility threshold $U_{threshold}$. Our proposed algorithm outperforms the other algorithms by at least 5.8% as POI utility threshold rises from 700 to 1400. Fig. 9 shows that the charging utility of the proposed algorithm and FC grows up nearly linearly with the utility threshold. This is because the increasement of threshold gives more improving space of the utility that makes the ascend trend.

For easy understanding, we visualize the sensor placement and energy allocation strategy as shown in Fig. 10. There are 50 POIs and the area is partitioned into 17*17=289 uniform grids, where we use original point (0,0) to denote the base station. By executing the proposed algorithm, we select 21 girds for sensor placement with corresponding energy allocation. The amount of energy allocated to sensors is indicated by color map. As the energy capacity of each sensor is divided into 20 pieces, we can place one sensor and charge half full energy if allocating 10 pieces of energy. Besides, we can place two sensors (one is full-charged and the other is half-charged) in a grid if the amount of allocated energy is 30 pieces. Moreover, more grids are selected near the original

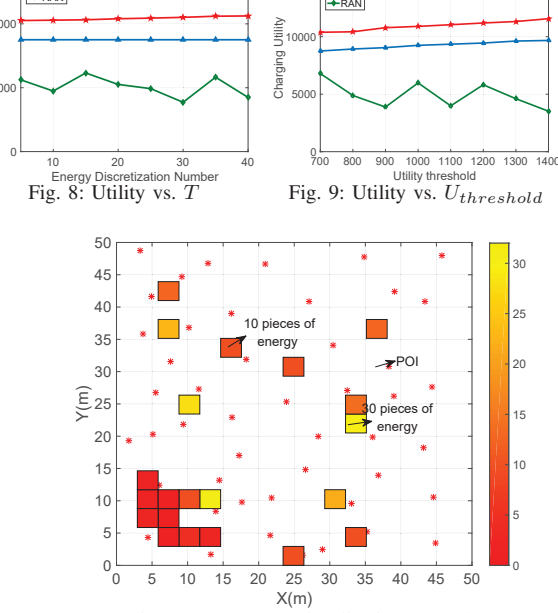


Fig. 10: A strategy visualization example

point because of the less traveling cost.

VII. FIELD EXPERIMENT

To further evaluate our proposed algorithm, we conduct field experiments to evaluate the performance.

As shown in Fig. 11, our testbed consists of a robot car with a TX91501 power transmitter produced by Powercast [29], rechargeable sensors and an AP connecting to a laptop to report the collected energy. We set 6 POIs with coordinates (1.5, 1.5), (1.8, 3.6), (4.2, 1.8), (3.4, 4.6), (2.4, 2.6) and (3, 1.6) in a 5m*5m square area of the office room. Then we can record the charging utility from deployed sensors. Sensors can harvest flexible energy via various charging duration for the fixed received power. The robot car moves at a speed of 0.3m/s. Thus, we can use time constraint to represent the energy budget. In our experiment, we restrict the executing time of the car to 5 minutes.

Fig. 12 shows a practical example of practical sensor placement and charging tour by executing our algorithm, where the mobile charger starts and ends at the bottom-left corner. The mobile charger visit 6 grids to provide energy and the charging time for each grid is denoted by the number in girds. We compare the charging utility between the proposed algorithm and FC by setting the utility threshold from 700 to 1400 as shown in Fig. 13. Thus our devised algorithm outperforms FC at least 7.8% and thus verifies the superiority.

VIII. CONCLUSION

This paper represents the first efforts towards joint sensors placement and mobile charging scheduling, where a mobile charger visits these deployed sensors for flexible energy transfer so as to improve the overall charging utility. We utilize the area partition and charging energy discretization methods to

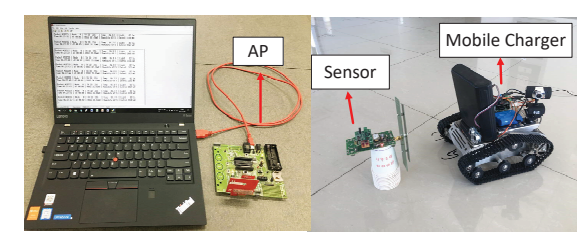


Fig. 11: Testbed: a mobile charger, AP and rechargeable sensor

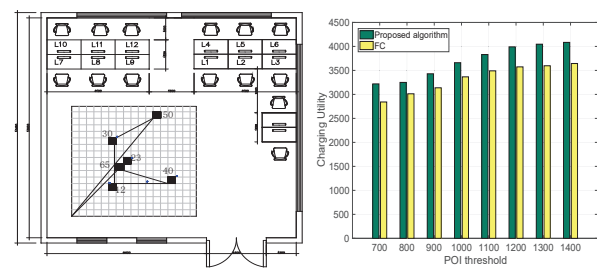


Fig. 12: Sensor placement and Fig. 13: Coverage utility vs. POI charging tour in the office room threshold

construct many virtual sensors with respect to various amount of harvested energy in a finite candidate positions. We present specific theoretical analysis to bound the discrete performance loss and prove the submodularity of the reformed objective function. Thus an efficient $(1-\varepsilon)/4(1-1/e)$ approximation algorithm is proposed to achieve a near optimal solution including deployed sensors with partial energy requirement and the closed charging tour. Finally, we evaluated the performance of the proposed algorithm against the full charging algorithm and our proposed algorithm outperforms well according to the results in the simulation and field experiment.

ACKNOWLEDGMENTS

Panlong Yang is the corresponding author. This research is partially supported by National key research and development plan 2017YFB0801702, NSFC with No. 61772546, 61625205, 61632010, 61751211, 61772488, 61520106007, Key Research Program of Frontier Sciences, CAS, No. QYZDY-SSW-JSC002, NSFC with No. NSF ECCS-1247944, and NSF CNS 1526638. NSF of Jiangsu For Distinguished Young Scientist: BK20150030, in part by the National Key R&D Program of China under Grant No. 2018YFB1004704, in part by the National Natural Science Foundation of China under Grant No. 61502229, 61872178, 61832005, 61672276, 61872173, and 61321491, in part by the Natural Science Foundation of Jiangsu Province under Grant No. BK20181251, in part by the Fundamental Research Funds for the Central Universities under Grant 021014380079.

REFERENCES

- C. Lin et al., "Tadp: Enabling temporal and distantial priority scheduling for on-demand charging architecture in wireless rechargeable sensor networks," *Journal of Systems Architecture*, vol. 70, pp. 26–38, 2016.
- [2] I. Cardei, "Energy-efficient target coverage in heterogeneous wireless sensor networks," in *Proc. INFOCOM Joint Conference of the IEEE Computer and Communications Societies*, 2006, pp. 1976–1984 vol. 3.
- [3] C. Zhu et al., "Review: A survey on coverage and connectivity issues in wireless sensor networks," *Journal of Network & Computer Applica*tions, vol. 35, no. 2, pp. 619–632, 2012.
- [4] Y. Shi et al., "On renewable sensor networks with wireless energy transfer," in *INFOCOM*, 2011 Proceedings IEEE. IEEE, 2011, pp. 1350–1358.

- [5] L. Fu et al., "Minimizing charging delay in wireless rechargeable sensor networks," in *INFOCOM*, 2013 Proceedings IEEE. IEEE, 2013, pp. 2922–2930.
- [6] X. Ye et al., "Charging utility maximization in wireless rechargeable sensor networks," Wireless Networks, vol. 23, no. 7, pp. 2069–2081, 2017
- [7] W. Liang et al., "Approximation algorithms for charging reward maximization in rechargeable sensor networks via a mobile charger," IEEE/ACM Transactions on Networking (TON), vol. 25, no. 5, pp. 3161–3174, 2017.
- [8] Y. Ma et al., "Charging utility maximization in wireless rechargeable sensor networks by charging multiple sensors simultaneously," IEEE/ACM Transactions on Networking, no. 99, pp. 1–14, 2018.
- [9] L. He et al., "On-demand charging in wireless sensor networks: Theories and applications," in Mobile Ad-Hoc and Sensor Systems (MASS), 2013 IEEE 10th International Conference on. IEEE, 2013, pp. 28–36.
- [10] H. et al., "Evaluating the on-demand mobile charging in wireless sensor networks," *IEEE Transactions on Mobile Computing*, no. 1, pp. 1–1, 2015.
- [11] A. Kaswan et al., "An efficient scheduling scheme for mobile charger in on-demand wireless rechargeable sensor networks," *Journal of Network* and Computer Applications, vol. 114, pp. 123–134, 2018.
- [12] C. Lin et al., "P2s: A primary and passer-by scheduling algorithm for ondemand charging architecture in wireless rechargeable sensor networks," *IEEE Trans. Veh. Technol*, vol. 66, no. 9, pp. 8047–8058, 2017.
- [13] L. C. et al., "Tsca: A temporal-spatial real-time charging scheduling algorithm for on-demand architecture in wireless rechargeable sensor networks," *IEEE Transactions on Mobile Computing*, vol. 17, no. 1, pp. 211–224, 2018.
- [14] G. A. Shah et al., "Exploiting energy-aware spatial correlation in wireless sensor networks," in *International Conference on Communication Systems Software and Middleware*, 2007. Comsware, 2007, pp. 1–6.
- [15] F. Bouabdallah et al., "Reliable and energy efficient cooperative detection in wireless sensor networks," Computer Communications, vol. 36, no. 5, pp. 520–532, 2013.
- [16] S. Zhang et al., "P 3: Joint optimization of charger placement and power allocation for wireless power transfer," in 2015 IEEE Conference on Computer Communications (INFOCOM). IEEE, 2015, pp. 2344–2352.
- [17] H. Dai et al., "Safe charging for wireless power transfer," IEEE/ACM Transactions on Networking, vol. 25, no. 6, pp. 3531–3544, 2017.
- [18] L. Li et al., "Radiation constrained fair wireless charging," in Sensing, Communication, and Networking (SECON), 2017 14th Annual IEEE International Conference on. IEEE, 2017, pp. 1–9.
- [19] H. Dai et al., "Radiation constrained scheduling of wireless charging tasks," *IEEE/ACM Transactions on Networking*, vol. 26, no. 1, pp. 314– 327, 2018.
- [20] Y. Shu et al., "Near-optimal velocity control for mobile charging in wireless rechargeable sensor networks," *IEEE Transactions on Mobile Computing*, vol. 15, no. 7, pp. 1699–1713, 2016.
- [21] Z. Dong et al., "Energy synchronized task assignment in rechargeable sensor networks," in Sensing, Communication, and Networking (SEC-ON), 2016 13th Annual IEEE International Conference on. IEEE, 2016, pp. 1–9.
- [22] P. Zhong et al., "Rcss: A real-time on-demand charging scheduling scheme for wireless rechargeable sensor networks," Sensors, vol. 18, no. 5, p. 1601, 2018.
- [23] L. Jiang et al., "On-demand mobile charger scheduling for effective coverage in wireless rechargeable sensor networks," in *International* Conference on Mobile and Ubiquitous Systems: Computing, Networking, and Services. Springer, 2013, pp. 732–736.
- [24] H. Dai et al., "Radiation constrained wireless charger placement," in IEEE INFOCOM 2016 - the IEEE International Conference on Computer Communications, 2016, pp. 1–9.
- [25] D. et al., "Optimizing wireless charger placement for directional charging," in INFOCOM 2017 IEEE Conference on Computer Communications. IEEE, 2017, pp. 1–9.
- tions, IEEE, 2017, pp. 1–9.
 [26] S. Khuller et al., "The budgeted maximum coverage problem," Information Processing Letters, vol. 70, no. 1, pp. 39–45, 1999.
- [27] D. Feillet et al., "Traveling salesman problems with profits," Transportation science, vol. 39, no. 2, pp. 188–205, 2005.
- [28] H. Zhang *et al.*, "Submodular optimization with routing constraints." in *AAAI*, vol. 16, 2016, pp. 819–826.
- [29] Powercast, "Online," http://www.powercastco.com/products/.